Biosensors and Bioelectronics 74 (2015) 718–724

Contents lists available at ScienceDirect

Biosensors and Bioelectronics

journal homepage: www.elsevier.com/locate/bios

A "signal-on" aptasensor for simultaneous detection of chloramphenicol and polychlorinated biphenyls using multi-metal ions encoded nanospherical brushes as tracers

Zhongdan Yan [a], Ning Gan [a,*], De Wang [a], Yuting Cao [a], Meng Chen [a], Tianhua Li [a], Yinji Chen [b]

[a] State Key Laboratory Base of Novel Functional Materials and Preparation Science, Faculty of Materials Science and Chemical Engineering, Ningbo University, Ningbo 315211, PR China
[b] Nanjing University of Finance and Economics, PR China

ARTICLE INFO

Article history:
Received 22 May 2015
Received in revised form
10 July 2015
Accepted 11 July 2015
Available online 16 July 2015

Keywords:
Multiplex determination
Chloramphenicols
Polychlorinated biphenyls
Metal ion tracer
Competitive-type displacement reaction

ABSTRACT

A "signal-on" aptasensor was developed for simultaneous detection of chloramphenicols (CAP) and polychlorinated biphenyl-72 (PCB72) with a novel multi-metal ions encoded nanospherical brushes as nanotracers. To construct the assay, the respective aptamer of CAP and PCB72 labeled magnetic gold nanoparticles as capture probes (aptamer-MGPs), and their complementary single strand DNA (s-DNA) encoded metal ions (Cd^{2+} and Pb^{2+}) on nanospherical branched polyethylene imine brushes as tracers (s-DNA-MSPEIs), were simultaneously synthesized. After that, the capture probe and tracers were connected through a hybridization reaction between s-DNA and aptamers. In the presence of CAP and PCB72, the analytes could react with the aptamers on capture probes and release the tracers into supernatant after magnetic separation. The released tracers with metal ions (Cd^{2+} and Pb^{2+}) could be simultaneously detected through the square wave voltammetry (SWV) without acid dissolution, which can switch the signals of the biosensor to "on" state. Under optimal conditions, the assay could detect CAP and PCB72 as low as 0.3 pg mL^{-1} with the dynamitic range from 0.001 to 100 ng mL^{-1} and exhibited excellent selectivity. More importantly, the strategy can be extended easily to other targets after changing the corresponding aptamers and other metal ions tracers, which provides a promising and facile approach in multiplex detection of ultra-trace level of pollutants in food safety without more complex separation and washing steps.

1. Introduction

In food safety analysis, it is crucial to develop a method for simultaneous detection of several harmful and bio-accumulative compounds which can cause health risks to humans and wildlife. As a broad-spectrum antibiotic, chloramphenicol (CAP) is widely used in animals as the growth promoters and the treatment of diseases. However, it has been found that the excessive levels of CAP which exists in fish, shrimp and pork have some side effects such as aplastic anemia, gray baby syndrome, and leukemia which would threaten public health (Yan et al., 2012; Yang and Zhao, 2014; Yadav et al., 2014). Polychlorinated biphenyls (PCBs) are a group of highly persistent organic compounds, which are used as additives in pesticides, paints, as well as sealants. It can be accumulated by millions of times in fish and mammals, which can induce serious neuroreproductive toxicity, immunotoxicity, and tumor promotion to human health (Mehta et al., 2012; Xu et al., 2012; Ottonello et al., 2014). Therefore, the two bio-accumulative compounds residues have designated tolerance levels for CAP of 0.3 μg kg^{-1} and PCBs that range between 0.2 and 3 μg kg^{-1} in food, and these residue limits are used to determine whether or not a food is safe to consume (Bangemann, 1994; Mehta et al., 2012). Thus, in the study, CAP, PCB72 were used as a model for detection in fish samples. Moreover, it's urgent to develop a kind of sensitive and quick assay to enable screen monitor of the residues of CAP and PCB72 together in food samples (Mehta et al., 2012; Yan et al., 2012; Yadav et al., 2014).

Various analytical methods and techniques are used for the determination of CAP or PCBs, including gas chromatography–mass spectrometry (Sapozhnikova and Lehotay, 2013; Ottonello et al., 2014), and high-performance liquid chromatography

* Corresponding author. Fax: +86 574 87609987.
E-mail addresses: ganning@nbu.edu.cn (N. Gan), caoyuting@nbu.edu.cn (Y. Cao).

http://dx.doi.org/10.1016/j.bios.2015.07.024
0956-5663/

(Posyniak et al., 2003; Yadav et al., 2014; Yang and Zhao, 2014; Silva et al., 2007). These traditional separation-based methods are sensitive, reliable and stable, but their high cost and complicated operation limit their application. Electrochemical biosensor has attracted considerable attention for its intrinsic advantages, such as, rapid response, ease to use, inexpensive instrumentation (Yan et al., 2012; Pilehvar et al., 2012; Borowiec et al., 2013; Pilehvar et al., 2014), which can also be employed in simultaneous determination by using several signal tracers (Liang et al., 2014).

However, to find high-sensitive and distinguishable multi-tracers is the key issue to achieve simultaneous analysis in the electrochemical assay. Quantum dots (Hansen et al., 2006a, 2006b), methylene blue (Jiang et al., 2015), ferrocene (Yang et al., 2014), thionine (Liang et al., 2014) have been widely used as the signal tracers in the traditional reports. Among them, the metallic nanoparticles or quantum dots have attracted much attention due to their extremely high sensitivity (Feng et al., 2012). Moreover, metal ions in the metallic nanoparticles, such as Cd^{2+}, Pb^{2+} and Zn^{2+} can be easily and simultaneously detected by stripping voltammetry, because of the different electrochemical oxidation–reduction potential. However, the complicated acid dissolution steps are usually indispensable to derive the metal ions out from the nanoparticles before detection which is time-consuming and toxic. (Feng et al., 2012; Xu et al., 2014). Thus, it is necessary to fabricate a preparation method to facilely immobilize metal ions on the tracers, and can be detected directly.

Nanostructures with amino-groups showed good adsorption and enrichment properties for Pd^{2+}, Cd^{2+}, Ni^{2+}, Co^{2+}, Cu^{2+}, and Ag^{+} (Yi et al., 2006). Therefore, it provided another simple strategy to immobilize metal ions on it as tracers. Herein, we reported the development of a sensitive assay system by using metal ions encoded nanospherical hyperbranched polyethylene imine brushes (MSPEIs) as signal carriers, and MSPEIs conjugated with s-DNA (s-CAP and s-PCB) were prepared as tracers for simultaneous detection of CAP and PCB72. The Pb^{2+} and Cd^{2+} were used as electrochemical tracers because of their different redox potential and strong binding capacity with amino-groups on spherical hyperbranched polyethylene imine brushes (SPEIs). In addition, SPEIs have many excellent properties over conventional carriers, such as the three-dimensional spherical structure with larger specific area, and can act as ideal supports for metal ions tracer loading while keeping their electrochemical activities. The loading process of metal ions, such as Cd^{2+} and Pb^{2+}, on SPEIs were greatly simplified, the metal ion probe could be detected directly through square wave voltammetry (SWV) without acid dissolution.

Another case being needed to overcome is to find a selective, stable, cheap probe to capture the targets, fabricate the facile multiplex electrochemical biosensor. Antibodies, which were widely used in electrochemical immunosensor as capture probes, always play the key roles due to their good selectivity and labeling features. However, they also display some shortcomings, such as expensive, instable in different production batches, easy to denature. Compared with antibodies, aptamers with higher affinity toward targets were used in this work. Aptamer have attracted substantial attention as recognition elements in bio-detections, owing to their easy preparation in batch by PCR, high stability and selectivity, facile modification capabilities over antibodies (Jiang et al., 2015; Wei et al., 2015). In this work, two aptamers respectively for CAP and PCB72, were simultaneously immobilized on magnetic gold nanoparticles (MGPs) to synthesis the capture probes to construct the electrochemical aptasensor without more complex separation and washing steps.

Herein, we designed a simple and efficient aptamer sensor for simultaneous detection of two bioaccumulative compounds in fish, CAP and PCB72 being used as a model, based on a novel metal ion tracers by coupling a competitive-type displacement reaction mode. In this assay, more metal dissolution, complex separation and washing steps were not required any more. Based on the complementary base-pairing reaction, MGPs with aptamers were initially hybrid with the s-DNA modified MSPEIs, leading to a decrease of the supernatant signal. Upon target CAP and PCB72 were introduced, a specific competitive-type displacement reaction for cDNA-MSPEIs tracers were carried out between aptamers-MGPs and target CAP and PCB72, leading to the release of s-DNA-MSPEIs tracers from aptamers-MGPs and increasing the amount of tracers in the supernatant, thus the signal was in its “on” state. Therefore, the target-induced “signal-on” aptasensor could be used for specific differentiate and quantification of two analytes simultaneously. The assay was also employed for detection of CAP and PCB72 in fishes.

2. Experiment

2.1. Reagents and apparatus

Tetraethyl orthosilicate (TEOS) (99.99%, Aldrich), (3-aminopropyl)-triethoxysilane (APTES), glutaraldehyde (25% aqueous solution), tris (2-carboxyethyl) phosphine hydrochloride (TCEP), CAP and PCB72 (in this paper, PCB72 was used as the template of PCBs (Mehta et al., 2012), and their chemical structure are provide in supporting information) were purchased from Sigma-Aldrich Co., Ltd. (St. Louis, MO, USA). $HAuCl_4$, 6-Mercapto-1-hexanethiol (MH) were purchased from Aladdin Co., Ltd. (Shanghai, China). $Cd(NO_3)_2$, $Pb(NO_3)_2$, Tris, sodium citrate, and all other chemicals were of analytical reagent grade, and doubly distilled water was used in all the experiments. All oligonucleotides were obtained from Sangon Biological Engineering Technology & Services Co., Ltd. (Shanghai, China) and purified using high performance liquid chromatography, and the sequences of the oligonucleotides were given below:

CAP aptamer: SH-$(CH_2)_6$-ACT TCA GTG AGT TGT CCC ACG GTC GGC GAG TCG GTG GTA G

PCB72 aptamer: SH-$(CH_2)_6$-CAC TCG GAC CCC ATT CTC CTT CCA TCC CTC ATC CGT CCA C

s-CAP: NH_2-$(CH_2)_6$-ACC ACC GAC TCG CCG

s-PCB72: NH_2-$(CH_2)_6$-GGA CGG ATG AGG GAT

All electrochemical coding assay measurements were performed on a CHI 620D Electrochemical Workstation (CHI, Austin, TX, USA). A glassy carbon electrode (GCE, 3 mm diameter) was used as working electrode, with Ag/AgCl and platinum wire acted as the reference electrode and auxiliary electrode, respectively. Infrared spectra were recorded with a Nicolet 6700 FT-IR spectrophotometer (Madison, Wisconsin, USA). The transmission electron microscopic (TEM) image was obtained with a H600 transmission electron microscope (Hitachi, Tokyo, Japan).

2.2. Preparation of distinguishable tracers

Amino-functionalized silica nanoparticles were prepared according to the Stöber method (Yang et al., 2010; An et al., 2007; Kim et al., 2006; Rao et al., 2005) (details in Supporting information). Next, 10 mg of amino-functionalized silica nanoparticles (SiO_2) were placed in 2 ml of 2.5% glutaraldehyde and phosphate buffer solution (PBS) at pH 7.4 activated for 1 h at room temperature (Lopez-Gallego et al., 2005; Zhang et al., 2011). The activated SiO_2 were incubated with 1 ml 1% of PEI and reacted for 2 h, the excess PEI was removed by centrifugation to obtain the SPEIs. Then, the prepared SPEIs was dispersed in 1.2 mL of 10 mM $Cd(NO_3)_2$ (or 1.6 ml of 10 mM $Pb(NO_3)_2$) aqueous solution and reacted for 12 h under gently stirring (Yi et al., 2006). After

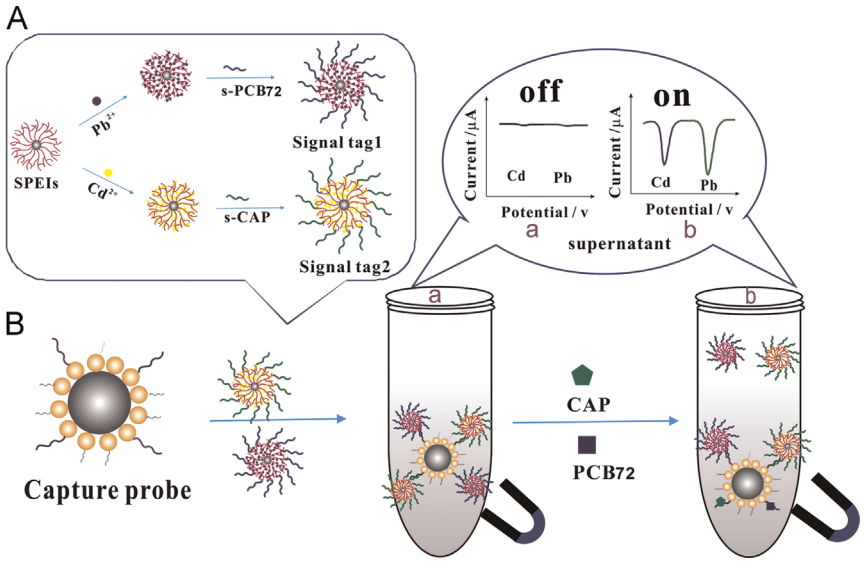

Scheme 1. Schematic representation of simultaneous electrochemical detection of chloramphenicols and polychlorinated biphenyls based on metal ions encoded nanospherical brushes tracers.

centrifugated and washed for three times, the obtained MSPEIs were redispersed in 2 mL of PBS, that containing about 2.5% glutaraldehyde, and with gently stirring for 1 h. Then MSPEIs were incubated with s-PCB and s-CAP at room temperature, respectively. Free s-PCB and s-CAP were removed by centrifugation and were washed with PBS for several times, and the obtain conjugates were dispersed with PBS to store for further use at 4 °C. The fabrication of the distinguishable tracers was illustrated in Scheme 1A.

2.3. Preparation of the capture probes

Magnetic gold nanoparticles (MGPs) were synthesized with our previously reported method (Yan et al., 2015). Briefly, 5 mg MGPs was transferred into 1 mL of PBS buffer that containing about 50 μL (1.0×10^{-6} M) of CAP and PCB72 aptamers. After being shaken gently for 16 h at room temperature, the MGPs-aptamer conjugates were formed and then incubated with 1 mM of MH to block the remaining binding sites at room temperature for 40 min. The conjugates were washed and separated with magnetic. Finally, the prepared conjugates (capture probe) were dispersed in PBS and stored at 4 °C for further use.

2.4. Fabrication of the biosensor

The analytical procedure involving a dual process was shown in Scheme 1B. The homologous amount of signal tracers were injected into the PBS including the capture probes. Then the hybridization steps took place at 37 °C for 2 h to form MGPs-aptamers-s-DNA-MSPEIs compounds (Yao et al., 2014). Then the unbound tracers were removed thoroughly by washing with the same buffer with an external magnet. Next, sample solutions containing various concentrations of CAP and PCB72 were injected into the above compounds in the binding buffer (50 mM Tris–HCl (pH 7.4), 100 mM NaCl, 5 mM KCl, 1 mM $MgCl_2$) (Wu et al., 2015), and the mixture were incubated for 55 min. After magnetic separation, the supernatant, containing various concentrations of the tracers was obtained. Then the supernatant was used for electrochemical detection. Blank experiments were performed without adding analytes in a similar way. Real sample analysis processed in accordance with the standard enzyme linked immunosorbent assay (ELISA) method (LOT: HE09001).

2.5. Electrochemical detection

To detect CAP and PCB72, square wave voltammetry (SWV) measurements were performed to track Cd^{2+} and Pb^{2+} by using the glassy carbon electrode. Briefly, 200 μL of detection solution (containing the released tracers) was added into 1800 μL HAc-NaAc (pH 4.0) buffer solutions. SWV measurement was carried out from −1.0 to −0.3 V following pulse amplitude of 25 mV and a potential step of 4 mV was performed to record the electrochemical responses related to the CAP and PCB72 concentrations, respectively.

3. Results and discussion

3.1. Characterization of the metal ions tagged nanospherical brushes

To achieve the aim to load high capacity of metal ions in MSPEIs assemblies, two important factors are to synthesize SiO_2 with good monodispersion as carrier and the SPEIs with a large number of amino groups. To fulfill the purposes, the characteristics of the nanoparticals before and after the PEI grafting reaction were measured by transmission electron microscope (TEM) images. Fig. 1A showed the morphology of as-prepared SiO_2, which has a similar surface morphology and good monodispersion with a diameter of about 100 nm. Fig. 1B showed a TEM image of SPEIs, displaying a clear core–shell structure with a uniform size distribution. The SiO_2 was surrounded by the PEI without aggregation. Energy dispersive spectrometer (EDS) and X-ray photoelectron spectroscopy (XPS) characterization were employed to further analyze the nanomaterials of the Pb^{2+}-SPEIs and Cd^{2+}-SPEIs, as shown in Fig. S1 (Supporting information). The characteristic peaks of Si, O, C, and N were simultaneously observed for SPEIs nanospheres. Meanwhile, as shown in Fig. S1 (B) and (C), the presence of cadmium and lead in the metal ion labeled SPEIs were confirmed. Both Si/Cd and Si/Pb nanoparticles displayed a Si_{2p} peak at 103.1 eV in the XPS spectra (Fig. S1D), which could be attributed to the Si–O groups. In addition, two Cd_{3d} peaks at 404.9/411.7 eV for Cd^{2+}-SPEIs nanoparticles (Fig. S1E), as well as two peaks of Pb_{4f} at 137.8/142.7 eV for Pb^{2+}-SPEIs were observed (Fig. S1F) (Qian et al., 2011), which were all attributed to complexation of amino complex (Zhu et al., 2012). From the above, the as-

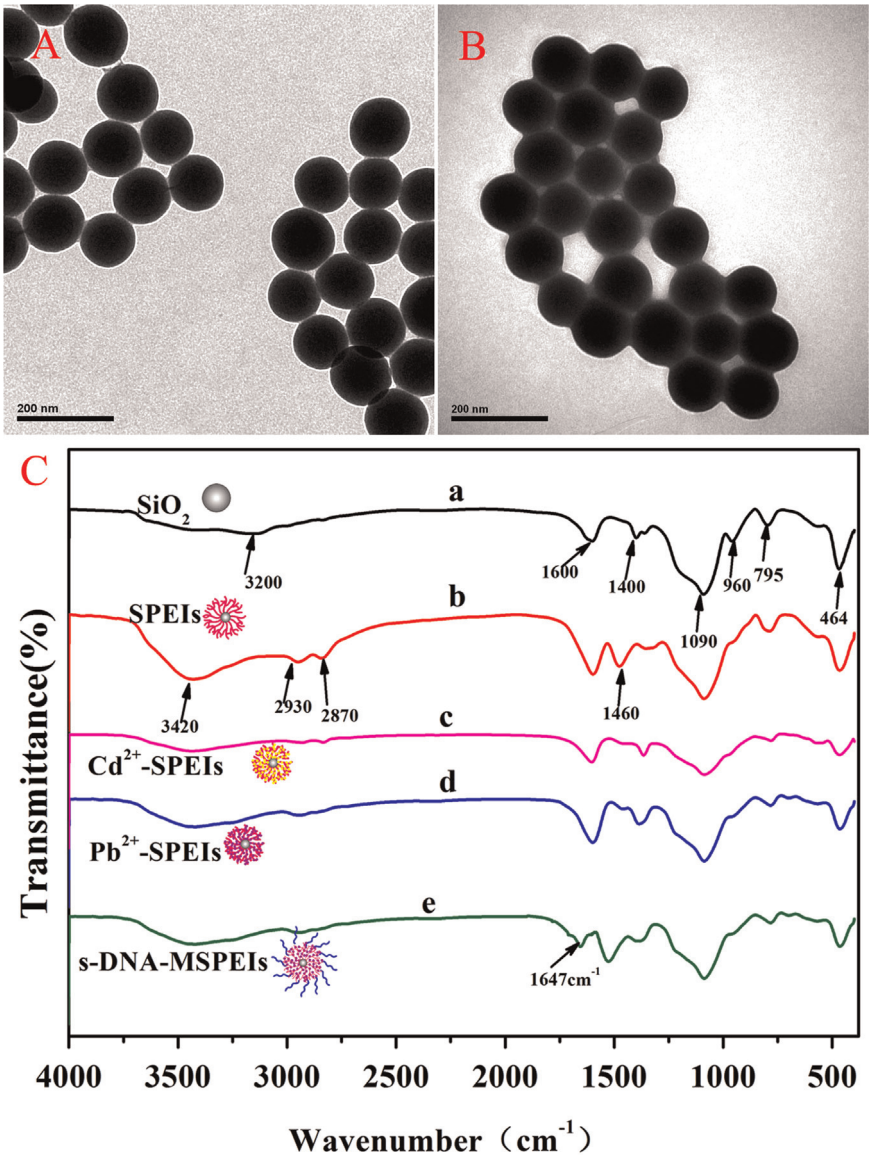

Fig. 1. TEM images of (A) silica nanoparticles and (B) SPEIs, (C) FT-IR spectra of (a) silica nanoparticles, (b) SPEIs, (c) Cd^{2+}-SPEIs, (d) Pb^{2+}-SPEIs, and (e) s-DNA-MSPEIs.

prepared SPEIs, Cd^{2+}-SPEIs, and Pb^{2+}-SPEIs were synthesized successfully.

Fourier transform infrared spectroscopy (FTIR) experiments were carried out to further demonstrate the formation of Pb^{2+}-SPEIs, Cd^{2+}-SPEIs and s-DNA-MSPEIs in Fig. 1C. Curve 'a' was the FT-IR spectra of SiO_2, some strong bands appear in the range of 1250–1000 cm^{-1} related to the Si–O–Si asymmetric stretching vibration, 795 cm^{-1} and 464 cm^{-1} can be contributed to the Si–O–Si swing and bending vibration, and the Si–OH bending bands appear at 960 cm^{-1}. There was also a broad peak at about 3200 cm^{-1}, which proved the existence of amino groups in the signal tag. When draped by PEI, the characteristic peak of SiO_2 at 960 cm^{-1} for Si–OH stretch disappeared (Yang et al., 2010), four characteristic absorption bands of PEI at 3420 cm^{-1} for N–H stretch, 2930 and 2870 cm^{-1} for C–H stretch, 1460 cm^{-1} for C–H bend appeared (Nayab et al., 2014; Zhang et al., 2012). Therefore, it could prove that PEI was successfully synthesized on the surface of SiO_2. In addition, compared curve 'c', 'd' with 'b' , both wavelength shift and shape change in peaks of N–H stretch and N–H bend vibration, indicate a strong interaction between amino groups of PEI and Pb^{2+} or Cd^{2+} (Zhang et al., 2012). A peak at 1647 cm^{-1}, shown in the spectra of that s-DNA immobilized on the MSPEIs, presumably represented the imine (N=C) Schiff-base produced by the amine-glutaraldehyde reaction (curve 'e') (Yang et al., 2010). The results indicated that the s-DNA-MSPEIs conjugates were successfully synthesied. Thus, the successful synthesis of Pb^{2+}-SPEIs, Cd^{2+}-SPEIs and s-DNA-MSPEIs could provide a chance for the development of MSPEIs-based sensor.

3.2. Characteristics of the biosensor using various biolabels

To clarify the advantages of electrochemical assay using s-DNA-MSPEIs as signal nanotracers, three types of tracers (i.e., s-DNA-SiO_2, s-DNA-PEI, and s-DNA-MSPEIs) were constructed for the comparison. Fig. 2A showed the SWV currents of three bioassay protocols after incubated with the same concentration of CAP and PCB72 analytes. Experimental results indicated that the bioassay system using s-DNA-MSPEIs as tracers exhibited a higher current than other labels. The observation might be attributed to the following several possible causes: (i) the SPEIs with numerous of amino-group that have strong binding capacity with metal ions, and (ii) the three-dimensional of SPEIs could obviously increase the immobilized amount of metal ions compared with that of two-dimensional original carriers, and enhance the sensitivity of the

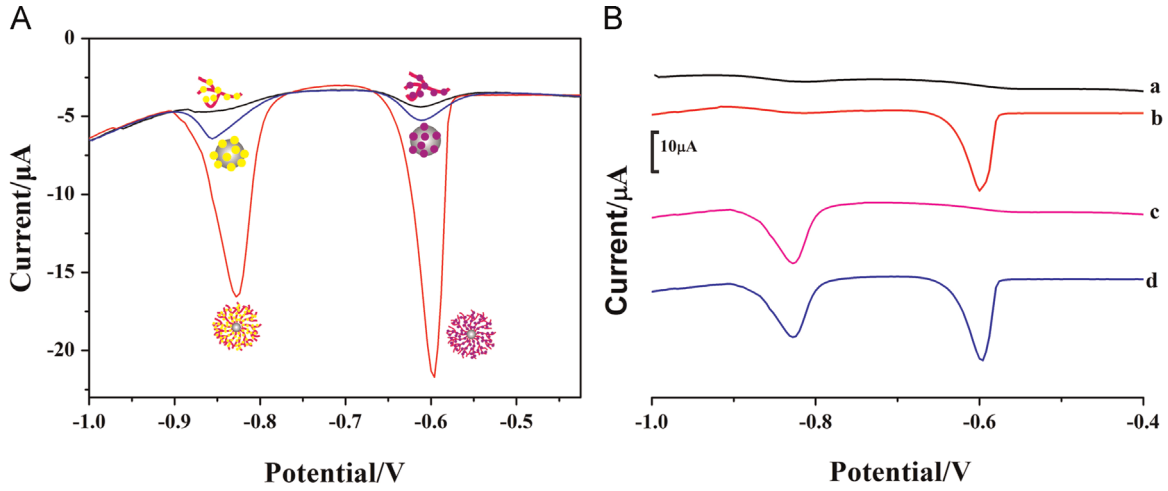

Fig. 2. (A) SWVs of three types of signal tag (a) s-DNA-MPEI, (b) s-DNA-$MSiO_2$, and (c) s-DNA-MSPEIs conducted biosensor. (B) SWV signals for the investigation of cross-reactivity.

bioassay.

An excellent biosensor for simultaneous multi-analyte detection must eliminate cross-reactivity between analytes. In this study, two different signal tracers (Pb^{2+} and Cd^{2+}) for PCB72 and CAP were hybridize with capture probes, the developed biosensor was incubated with CAP or PCB72 solution, or their mixture solutions, respectively. As shown in Fig. 2B, in the absence of target analytes, almost no peak current was observed (curve 2a). When the biosensor can only react with 100 ng mL^{-1} PCB72, the peak current of lead increased sharply, while the peak current of cadmium remained the same (curve 2b). When the biosensor was incubated with 100 ng mL^{-1} CAP alone, the peak current of cadmium obviously increased, while the peak current of lead remained its original response (curve 2c). Subsequently, when the two analytes were simultaneously reacted on the detection platform of the biosensor, two obviously distinguishable peaks being derived from cadmium and lead were obtained (curve 2d), and the simultaneous assay of two targets was in agreement with the single detection of the corresponding analyte. Meanwhile, Fig. S6 showed the SWVs, in the presence of a fixed concentration of CAP and a series of different concentrations of PCB72 or different CAP concentrations in the presence of a fixed concentration of PCB72. As expected, the cadmium stripping currents were unchanged with the decrease of PCB72 (Fig. S6A), while lead stripping currents were almost constant with the decrease of CAP (Fig. S6B). Moreover, the simultaneous addition of CAP and PCB72 resulted in the simultaneous increase of both metal peaks (Fig. S6C). Thus, the results indicated that simultaneous detection of CAP and PCB72 without cross reaction was possible. It can be considered specific toward each analyte by using the designed biosensor.

3.3. Optimization of experimental conditions

It is generally known that the pH value of detection solution has a great influence on the electrochemical performance of the biosensor (Feng et al., 2012). In order to obtain an optimal pH value, different pH of HAc/NaAc detection solution was prepared. As shown in Fig. S2 (A) and (B), with a pH of greater than 4.0, the peak current of Pb^{2+} decreased sharply with the increase of pH , while the variation of Cd^{2+} was more postponed. For the purpose of getting a well sensitivity for both metal ions reduction peak, HAc/NaAc of pH 4 was selected as the detection solution for CAP and PCB72 simultaneous determination.

The dosage of Pb^{2+} and Cd^{2+} in Scheme 1A was optimized to achieve the high binding capacity of metal ions and s-DNA on the platform of electrode (Fig. S3 in the Supporting information), the optimal volume of SPEIs to Pb^{2+} and Cd^{2+} were 5:4 and 5:3, respectively. Incubation time and temperature for aptamer-target reaction could affect the analytical performance of the sensor. According to the most previous reports (Wang et al., 2014, Dong et al., 2015), 7 °C was selected as the reaction temperature throughout the experiment. The incubation time of the electrochemical aptamer sensor was investigated at 37 °C, and the results were shown in Fig. S4. Because it would take some time to replace the tracers from the capture probes by targets, the peak current of Pb^{2+} and Cd^{2+} increased with the increasing of the reaction time. As the replace reaction of assay getting saturated, the peak current became stable after 55 min. Therefore, 55 min was chosen as the incubation time for the assay.

3.4. Analytical performance

Under the optimum conditions, the multi-tracers and capture probes based biosensor can be used for quantitative detection of CAP and PCB72 simultaneously. As shown in Fig. 3, once the CAP and PCB72 were added to the biosensor, a competitive-type displacement reaction was happened between the targets (CAP and PCB72) and the tracers, resulting in peak current increased due to the release of tracers. The binding constant of CAP-aptamer and PCB72-aptamer coated magnetic beads are $1.31 \times 10^6\ M^{-1}$ and $1.67 \times 10^7\ M^{-1}$, respectively (Mehta et al., 2011, 2012). With the increased concentration of CAP and PCB72, the current of lead and cadmium increased in the meantime, respectively. The current of the multiplexed electrochemical detection increased with the increasing concentrations of target analytes. The excellent linearity between the peak current and the logarithm of the analytes concentration were obtained in the range of 0.001–100 ng mL^{-1} (Fig. 3B and C). The limit of detection was found to be 0.3 pg mL^{-1} (at $S/N=3$), which were competitive with or even better than other reported single analyte determination assays (Table S1) (Wu et al., 2015; Yadav et al., 2014; Yang et al., 2014; Xu et al., 2012; Poli et al., 2009; Pilehvar et al., 2014). Consequently, a sensitive and simultaneous determination of the two analytes was achieved. The good performance of the biosensor should be attributed to the high metal ions binding capacity of SPEIs.

3.5. Specificity, precision, reproducibility and stability

To investigate the selectivity of the biosensor toward CAP and PCB72, various similar compounds were used, including

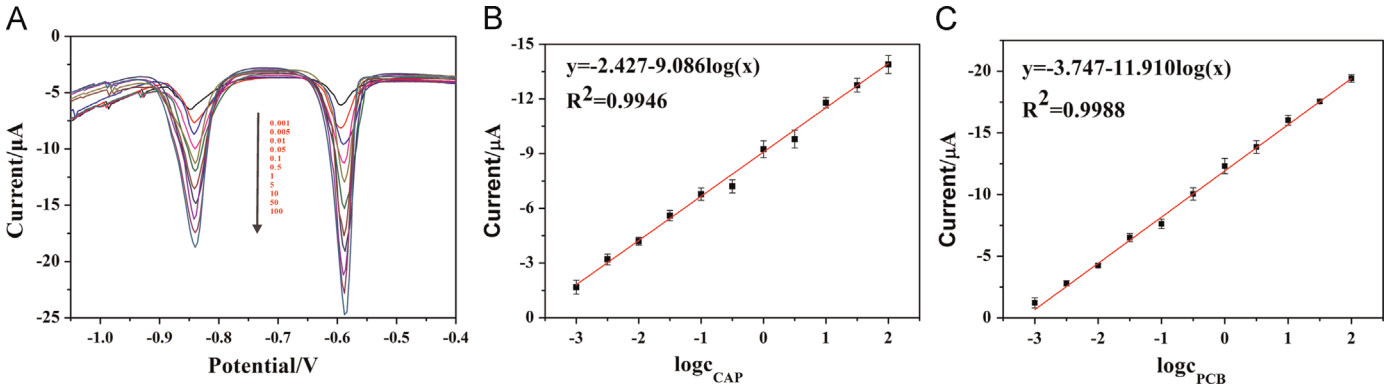

Fig. 3. (A) SWVs of CAP and PCB72 at different concentrations. (B) The calibration plot for CAP detection. (C) The calibration plot for PCB72 detection.

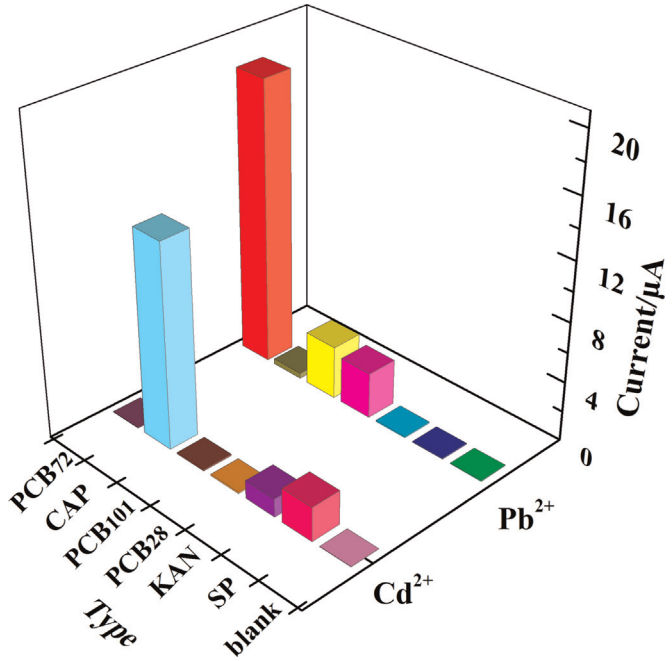

Fig. 4. The effects of interferences on the currents of the biosensors.

kanamycin, streptomycin, PCB 101 and PCB 28. As shown in Fig. 4, compared with the blank, no apparent change of current by the assay was observed. The other similar compounds showed almost negligible responses current of the biosensor even at a higher concentration (5.0 μg mL^{-1}) than that of CAP and PCB72 (100 ng mL^{-1}). This may be due to the high specificity and binding affinity between analytes and their aptamers. These results clearly demonstrated the high specificity of the electrochemical biosensors and can meet the requirement of screening of CAP and PCB72 in fish.

Next, the reproducibility of the developed biosensor for CAP and PCB72 samples was investigated with intra- and inter-assay precision. The intra-assay precision of the biosensor was evaluated by assaying one level of CAP and PCB72 for three similar measurements. Experimental results suggested that the relative standard deviation of the intra-assay were 5.9% and 7.6% for 100 ng mL^{-1} CAP and PCB72, respectively. While the inter-assay precision was estimated by determining one level of CAP and PCB72 with three bioassays made at the same form. The relative standard deviation of the inter assay were 6.7% and 8.8% for 100 ng mL^{-1} CAP and PCB72, which showed an acceptable repeatability. These results could be attributed to good uniformity and monodispersion of the SPEIs, the immobilizing of the same amount of Cd^{2+} or Pb^{2+} and the s-DNA on each SPEIs, and thus allowed the same immobilizing of Cd^{2+} and Pb^{2+} by each competitive-type displacement event at the specific CAP and PCB72 concentration. In addition, the stability of the biosensor was researched, and as much as 90% of the initial response was preserved after storage at 4 °C for 30 days. Therefore, the biosensor has acceptable storage stability, and is suitable as dual labels for simultaneous detection of CAP and PCB72 based on competitive-type displacement reaction.

3.6. Application in analysis of fish samples

To evaluate the analytical reliability and application potential of the proposed multiplexed biosensor, the protocol was employed to detect CAP and PCB72 content in three kinds of fish. The original concentrations of CAP and PCB72 in three fish samples were detected and listed in Table 1. In addition, different amounts of CAP and PCB72 were added into fish samples for the recovery tests. The recoveries for CAP and PCB72 with concentration of 0.025, 0.10, and 2.50 ng mL^{-1} were determined by standard addition methods. The results are listed in Table 1. It can be seen from the table, the recoveries were in an acceptable range from 92 to 110% for CAP and from 90% to 108% for PCB72, indicating good accuracy of the proposed method for sample. Therefore, the developed bioassay provides a promising application in quality control of food safety detection.

4. Conclusions

In summary, a simple and “signal-on” aptasensor was developed for simultaneous determination of CAP and PCB72 as model in fish using metal ions-loaded spherical branched polyethylene imine brushes (SPEIs) as tracers. The metal ions could conjugate with SPEIs through the amino-groups of PEI, and the metal ion tracers could be directly detected through SWV. More importantly, the competitive-type displacement method can be successfully conducted as a one-step incubation reaction with analytes and does not require more complex separation and washing steps. This work not only focuses on target CAP and PCB72, it can also be easily extended for other biological detection through the substitution of the appropriate aptamers.

Acknowledgments

This work was supported by the Natural Science Foundation of

Table 1
Recovery results for the detection of CAP and PCB72.

Samples	Found (ng mL^{-1})		Added (ng mL^{-1})		Detection (ng mL^{-1})		Recovery (%)	
	CAP	PCB72	CAP	PCB72	CAP	PCB72	CAP	PCB72
Grass carp		ND	0.025	0.025	0.070	0.027	97.2 ± 4.3	108.0 ± 3.6
	0.047 ± 0.002							
		ND	0.100	0.100	0.159	0.095	106.7 ± 5.2	95.0 ± 5.2
	0.049 ± 0.005							
		ND	2.500	2.500	2.430	2.480	95.6 ± 3.2	99.2 ± 7.1
	0.040 ± 0.007							
Snakehead			0.025	0.025	0.071	0.038	101.4 ± 6.1	95.0 ± 4.5
	0.045 ± 0.009	0.015 ± 0.003						
			0.100	0.100	0.159	0.098	100.0 ± 3.4	90.7 ± 7.3
	0.059 ± 0.003	0.008 ± 0.005						
			2.500	2.500	2.535	2.453	99.2 ± 4.4	97.6 ± 3.5
	0.055 ± 0.004	0.013 ± 0.007						
Crucian		ND	0.025	0.025	0.133	0.023	100.7 ± 4.2	92.0 ± 6.2
	0.107 ± 0.004							
		ND	0.100	0.100	0.192	0.091	102.7 ± 5.7	91.0 ± 4.5
	0.087 ± 0.003							
		ND	2.500	2.500	2.595	2.420	99.6 ± 6.1	96.8 ± 5.2
	0.105 ± 0.002							

ND: not found.

Zhejiang Province and Ningbo (Y15B050008, LY13C200017, 2013A610241, 2014A610184, 2013A610163, 201005016, and 2013C37033), the non-profit project funded by State Administration of Grain (201313010) and a project funded by the Priority Academic Program Development of Jiangsu Higher Education Institutions (PAPD), the excellent paper of graduate students cultivation fund from the Ningbo University (PY2014018), and the K.C. Wong Magna Fund from Ningbo University.

Appendix A. Supplementary material

Supplementary data associated with this article can be found in the online version at http://dx.doi.org/10.1016/j.bios.2015.07.024.

References

An, Y., Chen, M., Xue, Q., Liu, W., 2007. J. Colloid Interface Sci. 311, 507–513.
Bangemann, M., 1994. Commission Regulation (EC) No 1430/94. Official Journal of the European Communities: Brussels, Belgium.
Borowiec, J., Wang, R., Zhu, L., Zhang, J., 2013. Electrochim. Acta 99, 138–144.
Dong, H., Meng, X., Dai, W., Cao, Y., Lu, H., Zhou, S., Zhang, X., 2015. Anal. Chem. 87, 4334–4340.
Feng, L.-N., Bian, Z.-P., Peng, J., Jiang, F., Yang, G.-H., Zhu, Y.-D., Yang, D., Jiang, L.-P., Zhu, J.-J., 2012. Anal. Chem. 84, 7810–7815.
Hansen, J.A., Mukhopadhyay, R., Hansen, J.Ø., Gothelf, K.V., 2006a. J. Am. Chem. Soc. 128, 3860–3861.
Hansen, J.A., Wang, J., Kawde, A.N., Xiang, Y., Gothelf, K.V., Collins, G., 2006b. J. Am. Chem. Soc. 128, 2228–2229.
Jiang, B., Li, F., Yang, C., Xie, J., Xiang, Y., Yuan, R., 2015. Anal. Chem. 87 (5), 3094–3098.
Kim, M.I., Ham, H.O., Oh, S.-D., Park, H.G., Chang, H.N., Choi, S.-H., 2006. J. Mol. Catal. B Enzym. 39, 62–68.
Lopez-Gallego, F., Betancor, L., Mateo, C., Hidalgo, A., Alonso-Morales, N., Dellamora-Ortiz, G., Guisan, J.M., Fernandez-Lafuente, R., 2005. J. Biotechnol. 119, 70–75.
Liang, R.P., Tian, X.C., Qiu, P., Qiu, J.D., 2014. Anal. Chem. 86, 9256–9263.
Mehta, J., Van Dorst, B., Rouah-Martin, E., Herrebout, W., Scippo, M.L., Blust, R., Robbens, J., 2011. J. Biotechnol. 155, 361–369.
Mehta, J., Rouah-Martin, E., Van Dorst, B., Maes, B., Herrebout, W., Scippo, M.L., Dardenne, F., Blust, R., Robbens, J., 2012. Anal. Chem. 84, 1669–1676.
Nayab, S., Farrukh, A., Oluz, Z., Tuncel, E., Tariq, S.R., ur Rahman, H., Kirchhoff, K., Duran, H., Yameen, B., 2014. ACS Appl. Mater. Interfaces 6, 4408–4417.
Ottonello, G., Ferrari, A., Magi, E., 2014. Food Chem. 142, 327–333.
Posyniak, A., Zmudzki, J., Niedzielska, J., 2003. Anal. Chim. Acta 483, 307–311.
Poli, D., Caglieri, A., Goldoni, M., Castoldi, A.F., Coccini, T., Roda, E., Vitalone, A., Ceccatelli, S., Mutti, A., 2009. J. Chromatogr. B 877 (8–9), 773–783.
Pilehvar, S., Mehta, J., Dardenne, F., Robbens, J., Blust, R., De Wael, K., 2012. Anal. Chem. 84, 6753–6758.
Pilehvar, S., Ahmad Rather, J., Dardenne, F., Robbens, J., Blust, R., De Wael, K., 2014. Biosens. Bioelectron. 54, 78–84.
Qian, J., Dai, H., Pan, X., Liu., S., 2011. Biosens. Bioelectron. 28 (1), 314–319.
Rao, K.S., El-Hami, K., Kodaki, T., Matsushige, K., Makino, K., 2005. J. Colloid Interface Sci. 289, 125–131.
Silva, E., Mascini, M., Centi, S., 2007. Anal. Lett. 40, 1371–1385.
Sapozhnikova, Y., Lehotay, S.J., 2013. Anal. Chim. Acta 758, 80–92.
Wang, H., Jiang, X., Wang, X., Wei, X., Zhu, Y., Sun, B., Su, Y., He, S., He, Y., 2014. Anal. Chem. 86, 7368–7376.
Wei, Y., Chen, Y., Li, H., Shuang, S., Dong, C., Wang, G., 2015. Biosen. Bioelectron. 63, 311–316.
Wu, S., Zhang, H., Shi, Z., Duan, N., Fang, C., Dai, S., Wang, Z., 2015. Food Control 50, 597–604.
Xu, S., Yuan, H., Chen, S., Xu, A., Wang, J., Wu, L., 2012. Anal. Biochem. 423, 195–201.
Xu, T., Jia, X., Chen, X., Ma, Z., 2014. Biosens. Bioelectron. 56, 174–179.
Yi, Y., Wang, Y., Ye, F., 2006. Colloid Surf. A 277, 69–74.
Yang, G., Wu, J., Xu, G., Yang, L., 2010. Colloid Surf. B 78, 351–356.
Yan, L., Luo, C., Cheng, W., Mao, W., Zhang, D., Ding, S., 2012. J. Electroanal. Chem. 687, 89–94.
Yadav, S.K., Agrawal, B., Chandra, P., Goyal, R.N., 2014. Biosens. Bioelectron. 55, 337–342.
Yang, C., Dou, B., Shi, K., Chai, Y., Xiang, Y., Yuan, R., 2014. Anal. Chem. 86 (23), 11913–11918.
Yang, G., Zhao, F., 2014. Biosens. Bioelectron. 64, 416–422.
Yao, G.-H., Liang, R.-P., Yu, X.-D., Huang, C.-F., Zhang, L., Qiu, J.-D., 2014. Anal. Chem. 87, 929–936.
Yan, Z., Gan, N., Zhang, H., Wang, D., Qiao, L., Cao, Y., Li, T., Hu, F., 2015. Biosens. Bioelectron. 71, 207–213.
Zhang, Y., Zhang, Y., Jiang, J., Li, L., Yu, C., Hei, T., 2011. Appl. Surf. Sci. 257, 2712–2716.
Zhang, Y., Liu, J.M., Yan, X.P., 2012. Anal. Chem. 85, 228–234.
Zhu, Y., Hu, J., Wang, J., 2012. J. Hazard Mater. 221–222, 155–161.